JOURNAL OF CATALYSIS 62, 1–12 (1980)

The Oxidation of Carbon Monoxide over the (110) Surface of Iridium[1]

J. L. TAYLOR,[2] D. E. IBBOTSON, AND W. H. WEINBERG[3]

Division of Chemistry and Chemical Engineering, California Institute of Technology, Pasadena, California 91125

Received June 28, 1978; revised June 18, 1979

The heterogeneously catalyzed reaction of gaseous CO and O_2 to form CO_2 over Ir(110) has been studied, through measurements of the steady-state rate of CO_2 production, by mass spectrometry for surface temperatures between 300 and 1000 K, and for partial pressures of the reactants between 10^{-8} and 3×10^{-6} Torr. The rate expressions developed from a previous analysis of transient reactions were combined into a model that both qualitatively and quantitatively predicts trends in the steady-state measurements. However, the following four phenomena limit the applicability of this model: (1) The activation energies for CO desorption and CO oxidation depend markedly upon the composition of the adlayer on the surface. (2) Diffusion in the adlayer may limit the rates of CO desorption and CO oxidation, but this effect can be included empirically in the rate expression. (3) The catalyst surface is oxidized at temperatures where the steady-state rate of CO oxidation is rapid, i.e., a second species of atomically adsorbed oxygen forms irreversibly near 700 K. (4) Hysteresis in the rate of production of CO_2 with temperature occurs in the steady-state reaction.

INTRODUCTION

Steady-state rates of CO_2 production at low pressures ($< 10^{-5}$ Torr) have been measured as a function of surface temperature for several platinum metal catalysts (*1–7*). The rate of production is observed to increase rapidly with temperature until a maximum is reached near 600 K and then to decrease slowly at higher temperatures. In the regime where the rate increases with temperature, the desorption of chemisorbed CO and the subsequent competitive adsorption of oxygen and CO have been thought to be the rate-limiting steps since Langmuir first described this reaction (*1*). However, the elementary reaction that depicts the combination of oxygen and CO to form CO_2 has been a subject of controversy until recently (*6*). Although other mechanisms have been suggested (*8, 9*), the reaction of chemisorbed oxygen atoms with either chemisorbed or physically adsorbed CO molecules is thought to be the most probable path for CO oxidation (*1*). In the first case, termed the Langmuir–Hinshelwood (L–H) reaction, the rate of oxidation is proportional to the concentration of chemisorbed CO molecules; in the second case, termed the Eley–Rideal (E–R) reaction, the rate is proportional to the partial pressure of CO. In either instance, the rate is proportional to the coverage of chemisorbed oxygen atoms. At first, the dominant path for CO oxidation was thought to be the E–R reaction (*1*). The decrease in the steady-state rate of CO_2 production with increasing surface temperature was attributed to a decrease in the coverage of oxygen (*2–4*). Early studies with modulated molecular beams (*10, 11*) demonstrated that the decrease in the rate with temperature above 600 K could be explained only by the L–H reaction, for the coverage of CO, rather than oxygen, decreased with increasing temperature. A subsequent study with molecular beams (*6*) showed that CO oxidation on Pd(111) occurs through the L–H mechanism for surface temperatures below 600 K. Moreover, the oxidation of CO obeys the L–H reaction on Ir(111) (*12, 13*). Hence, the adsorption of

[1] Supported by the National Science Foundation under Grant DMR77-14976.

[2] Present address: Proctor and Gamble Company, Miami Valley Laboratories, Cincinnati, Ohio 45247.

[3] Camille and Henry Dreyfus Foundation Teacher–Scholar.

0021-9517/80/030001-12$02.00/0

oxygen and CO, the desorption of CO, and the L–H reaction to form CO_2 are the four elementary reactions that may limit the rate of CO oxidation over the platinum metal catalysts. For surface temperatures between 300 and 1000 K, where the steady-state rate is greatest at low pressures, the E–R reaction and the desorption of oxygen and CO_2 are thought to affect the rate to second order at most (*1*, *6*).

The present study of CO oxidation over Ir(110) was undertaken to supplement those of earlier investigations and to model the dependence of the steady-state rate of CO_2 production under various conditions. Much of the preliminary modeling of the steady-state rates of CO oxidation has utilized transient studies as presented in a previous paper (*14*). These transient studies by thermal desorption mass spectrometry focused on the following: (1) the dependence of the rate expressions for CO desorption and CO oxidation upon the composition of the adlayer; and (2) the competitive adsorption of CO and oxygen (*14*). The present work used a mass spectrometer to monitor the steady-state rate of CO_2 production. In these studies, the partial pressures of the reactants, CO and O_2, were varied between 10^{-8} and 3×10^{-6} Torr, and the temperature of the single-crystal catalyst was varied between 300 and 1000 K. To determine how ordering phenomena influence the oxidation rate, the structure of the chemisorbed layer was investigated with LEED. An interpretation of steady-state oxidation rates will be presented based on the kinetic expressions which were developed earlier (*14*).

2. EXPERIMENTAL DETAILS

The experiments were conducted in a stainless-steel bell jar with a base pressure below 2×10^{-10} Torr. Partial pressures in the steady-state reactions were measured with a quadrupole mass spectrometer. The order of the overlayer during steady-state reactions was assessed by LEED. The substrate, which was held on a precision manipulator by two 10-mil Ta wires, could be cooled with liquid nitrogen or heated resistively. The temperature of the substrate was measured with a Pt–Pt/10% Rh thermocouple. The intensity from the mass spectrometer and the EMF from the thermocouple were recorded digitally by a PDP-11/10 computer (*15*), but they are presented in analog form for convenience.

The catalyst was cut from a single crystal of Ir and was polished within 1° of the (110) orientation. Carbon was removed from the surface through a series of oxidation and reduction cycles, whereas oxygen was removed by annealing the substrate above 1600 K. Prior to each experiment, the surface was free from impurities with 0.01 ml (where 1 ml = 10^{15} cm^{-2}), as judged by Auger spectroscopy.

Although CO does not dissociate on Ir(110) at low pressures below 1300 K (*16*), the measurement of steady-state oxidation rates was complicated by the formation of a surface oxide at temperatures where the rate of oxidation is rapid (*17*). The oxide is distinct chemically from chemisorbed oxygen, and it is less reactive to reduction by CO (*14*). When a surface that is covered with chemisorbed oxygen is heated to 700 K, the oxide forms irreversibly with a saturation coverage of 0.25 ± 0.05 ml, but decomposes by annealing the surface above 1600 K. Since the presence of the surface oxide is known to affect the chemisorption of CO (*16*) and oxygen (*17*) on Ir(110), experiments were performed with both clean and oxidized surfaces of Ir(110) for the transient experiments mentioned (*14*) and the present steady-state experiments.

The mass spectrometer was used to monitor steady-state rates of CO_2 production as a function of surface temperature and of the composition of the reactant gas. The total pressure of the reactants was varied between 10^{-7} and 3×10^{-6} Torr, whereas the partial pressure of each reactant was varied between 10^{-8} and 3×10^{-6} Torr. The steady-state rates of CO_2 production were measured in the following way. A clean Ir(110) crystal at 300 K was exposed first to

CO. Oxygen was not admitted into the reactor until the surface had been exposed to 100 liters of CO. Following this exposure, the surface is covered with CO, which is typically the situation at steady state as is shown in the following section. After the partial pressures of CO, O_2, and CO_2 had equilibrated, the partial pressure of each gas was measured. To obtain reaction rates, the partial pressure of CO_2 was measured as the temperature of the surface was varied at a rate of 80 K min^{-1}. The measured oxidation rate at any temperature did not vary for slower heating rates. The temperature first was increased to 1000 K and then was returned to 300 K. As the temperature of the surface changed, the partial pressures of the reactants, CO and O_2, were not monitored since these could be determined directly from the change in the partial pressure of CO_2. Moreover, the extents of reaction were small, less than 20%, so that these partial pressures did not change significantly.

3. STEADY-STATE RATES OF CO_2 PRODUCTION

The steady-state rate of CO_2 production (R_r, molecules cm^{-2} s^{-1}) was measured as a function of the surface temperature (T) and the partial pressures (P_{CO} and P_{O_2}) of the reactants, CO and O_2. Representative data for total pressures (P_T) of 3.0×10^{-7} and 3.0×10^{-6} Torr are shown in Fig. 1. Oxidation rates were measured for total pressures of 1.0×10^{-7} and $1.0\ 10^{-6}$ Torr also. For each total pressure, the ratio of the CO partial pressure to the O_2 partial pressure ($Q \equiv$

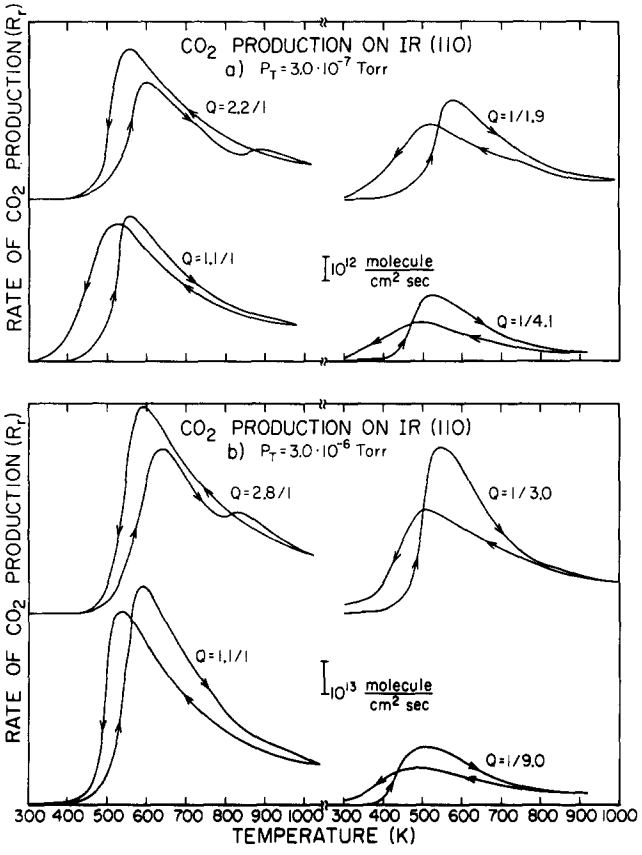

FIG. 1. Steady-state rates of CO_2 production as a function of the surface temperature with the ratio of the partial pressures of the reactants ($Q = P_{CO}/P_{O_2}$) as a parameter. Data are shown for total pressures of: (a) 3.0×10^{-7}, and (b) 3.0×10^{-6} Torr. The arrows on the curves point to the right if the temperature is increasing and to the left if the temperature is decreasing.

P_{CO}/P_{O_2}) was varied between 0.1 and 10 in separate experiments, which will be referred to as cycles. The arrows shown in Figs. 1 and 2 for each cycle point to the right if the surface temperature is increasing and to the left if the temperature is decreasing. Since typically less than 10% of either reactant gas was converted to CO_2 in these experiments, the ratio Q did not vary significantly with surface temperature. The values of Q shown in Fig. 1 were fixed at 300 K.

Several qualitative features are common among the cycles shown in Fig. 1. The variation in the steady-state rate with the surface temperature for any cycle is similar to that reported for CO oxidation over other surfaces of the platinum metals (*1–7*). A maximum in the rate appears near 600 K. At this temperature, CO begins to desorb rapidly from the platinum metals, suggesting that CO desorption limits the oxidation rate at lower temperatures (*1*). On Ir(110), the temperature associated with the maximum rate is independent of the total pressure in the gas phase (at least below approximately 10^{-5} Torr), but it is shifted to higher temperatures as Q is increased. From the transient studies of CO and oxygen on Ir(110), regardless of the coverage of oxygen, the rate of CO adsorption during the steady-state reaction is approximated by (*14*)

$$C_s \frac{d\theta_{CO}}{dt} = \frac{P_{CO}(1 - \theta_{CO})^2}{(2\pi M_{CO} k T_g)^{1/2}}, \qquad (1)$$

where C_s, θ_{CO}, M_{CO}, k, and T_g are the concentration of adsites (10^{15} cm^{-2}), the fractional coverage of CO, the molecular weight of CO, Boltzmann's constant, and the gas-phase temperature (taken as 300 K,), respectively. Since the rate of CO adsorption [Eq. (1)] increases with Q, this shift is further indication that the desorption of CO limits the rate below 600 K. Two features, which generally are not reported for CO oxidation, appear in the cycles in Fig. 1: (i) A second local maximum in the oxidation rate occurs near 800 K for larger values of Q; and (ii) the oxidation rates exhibit hysteresis as the catalyst temperature is varied. Moreover, a change in the maximum rate of CO_2 production is associated with this hysteresis.

The hysteresis might result from the oxidation of the surface since the rates of several elementary reactions in the overall oxidation differ for clean and oxidized Ir(110) (*14*). To test this hypothesis, the maximum temperature of the catalyst, rather than Q, was varied among cycles. Several cycles for values of Q of 2.7/1 and 1/4.4 are shown in Fig. 2. In these experiments, the surface was cleaned *before the first cycle only*. The total pressure was 1.0×10^{-6} Torr. In the absence of CO, the surface is oxidized near 700 K (*17*), but, in the presence of CO, the surface may be oxidized at higher temperatures since the processes of CO oxidation and oxide formation may compete for chemisorbed oxygen.

For a value of Q of 2.7, the maximum rate of oxidation did not change if the maximum surface temperature in the first cycle was maintained below 750 K. However, hysteresis still occurred, as is shown in Fig. 2a. This hysteresis appears not to be time dependent; the oxidation rates at the two maxima were stable over 30 min, which was the longest time that the stability was tested. If after the surface temperature had returned to 300 K and the reactant gases were evacuated, CO was the only desorption product observed when the surface was heated to 1800 K. During the second cycle, the second local maximum in the steady-state rate appeared when the surface temperature first exceeded 850 K but did not occur subsequently. As the temperature was returned to 300 K, the maximum rate of CO_2 production increased. Moreover, the increase was irreversible since the rate at the maxima did not change in succeeding cycles so long as the sample was not cleaned. When the reactants were evacuated following the second or succeeding cycles, a (2×1) $p1g1$ LEED pattern, characteristic of CO chemisorption on

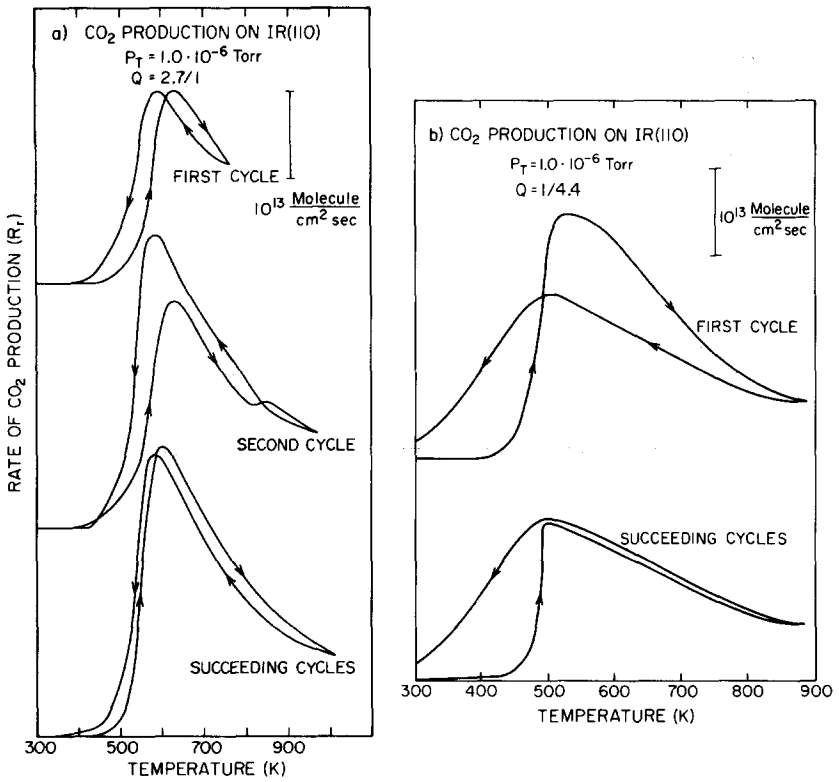

FIG. 2. Steady-state rates of CO_2 production as a function of surface temperature with the surface history as a parameter. Data are shown for a total pressure of 1.0×10^{-6} Torr and for ratios of the partial pressures of the reactants ($Q = P_{CO}/P_{O_2}$) of: (a) 2.7/1 and (b) 1/4.4. The arrows on the curves point to the right if the temperature is increasing and to the left if the temperature is decreasing.

oxidized Ir(110) only (*16*), was observed on the surface. Upon flashing the surface to 1800 K, CO, O_2, and CO_2 were desorbed so that the catalyst was oxidized during the second cycle, but not during the first cycle. Therefore, although the hysteresis cannot be attributed solely to oxide formation on the catalyst, the second local maximum in the steady-state rate with increasing temperature and the change in the maximum steady-state rate of CO_2 production are associated with oxide formation on the catalyst. Moreover, although the oxide layer may be reduced by CO (*14, 16*), at least a fraction of the oxide is stable between 300 and 1000 K while CO_2 is produced under steady-state conditions. For values of Q greater than 2, the hysteresis is less pronounced following the oxidation of the surface. Also, the maximum steady-state rate of CO_2 production is *increased* following the formation of the oxide. Both trends are evident in Fig. 2a.

Data for the experiment described above are shown in Fig. 2b, but here $Q(= P_{CO}/P_{O_2})$ is 1/4.4. After the catalyst temperature first exceeded 700 K, oxidation of the surface occurred, and it had to be cooled below 300 K to quench the production of CO_2. As before, the oxidation of the catalyst was verified both by LEED and by thermal desorption. As Q decreased, the oxide layer generally formed at lower temperatures. As shown in the curve for the first cycle, the maximum steady-state rate of CO_2 production was larger before the surface was oxidized. For values of Q less than 1, the maximum steady-state rate decreased after the surface was oxidized. Moreover, significant hysteresis was not observed for

temperatures above the maximum but was quite pronounced at lower temperatures. Again, hysteresis cannot be attributed solely to differences in the catalytic behavior on the clean and oxidized surfaces. Hysteresis is observed in cycles for which the surface is always clean, i.e., unoxidized, as in the first cycle in Fig. 2a, or always oxidized, as in succeeding cycles in Fig. 2b.

Hysteresis would appear in the CO oxidation rate if the kinetics of the elementary reactions that limit the steady-state rate vary nonlinearly in the coverage of either CO or oxygen. Hence, two or more minima in the total Gibbs energy, each associated with different coverages of reactants, may exist at any surface temperature. Although the Gibbs energy for one minimum may be substantially smaller than the energy for all others, a large activation energy may prevent the system from attaining the lowest possible Gibbs energy. The minimum that is entered as the temperature changes depends upon the composition of the adlayer prior to the change and, therefore, depends upon the rate and the sign of the change. The "steady-state" rates shown in Figs. 1 and 2 did not vary with heating rate as long as it was maintained below 4 K s^{-1}, but they did vary considerably with the sign of the heating rate. Although the two different rates at the same temperature were stable, the rates for larger values of Q tended to become unstable and fall rapidly for temperatures below 600 K as the surface was cooled. In this and other respects, the hysteresis reported for CO oxidation over polycrystalline Pt (7) is similar to that observed in this study.

LEED was not only useful for indicating that the surface was oxidized but was also useful for showing that chemisorbed oxygen clusters into islands when the steady-state rate of CO oxidation is large. On clean Ir(110), a $p(2 \times 2)$ pattern, which appears for oxygen coverages near 0.25 ml in the absence of CO, is formed for temperatures near the maximum in the steady-state rate. On oxidized Ir(110), a $c(2 \times 2)$ pattern, which appears for oxygen coverages between 0.2 and 0.6 ml in the absence of CO, formed for temperatures near the maximum also.

To obtain apparent activation energies for CO oxidation under steady-state conditions, the logarithm of the steady-state rate of production of CO_2 was plotted as a function of the reciprocal of the surface temperature for each cycle, as in Fig. 3. For all cycles shown, the surface was clean initially, but it was oxidized as the temperature was decreased (i.e., for curves with arrows pointing to the right). The slope of the linear part of each plot gives an apparent activation energy divided by the Boltzmann constant (E_a/k), whereas the intercept gives the logarithm of the apparent preexponential factor ($\ln \nu_a$), recognizing that the rate of production of CO_2 may be written as $R_r = \nu_a \exp(-E_a/RT)$, where T is the surface temperature.

In the region where the rate increases with temperature of the clean surface, the apparent activation energy (E_1) is between 13 and 16 kcal $mole^{-1}$, regardless of the total pressure and the value of Q. In the same region for the oxidized surface, the activation energy is between 5 and 20 kcal $mole^{-1}$, and tends to increase with Q. In the region where the oxidation rate decreases with temperature of clean or oxidized Ir(110), the apparent activation energy (E_2) is between -6 and -3 kcal $mole^{-1}$, regardless of the total pressure and the value of Q.

The apparent preexponential factors for the oxidation reaction may be related empirically to the reactant partial pressures (P_{CO} and P_{O_2}) by

$$\nu_a = \nu_i P_{CO}^{m} P_{O_2}^{n} \qquad (2)$$

where ν_i, m, and n are constants. In the region where the rate increases with temperature on the clean surface, the apparent preexponential factor is proportional to $P_{O_2}^2/P_{CO}$ ($= P_{O_2}/Q$), as shown in Fig. 4. For this region, the oxidation rate (R_r in molecules cm^{-2} s^{-1}) is given by

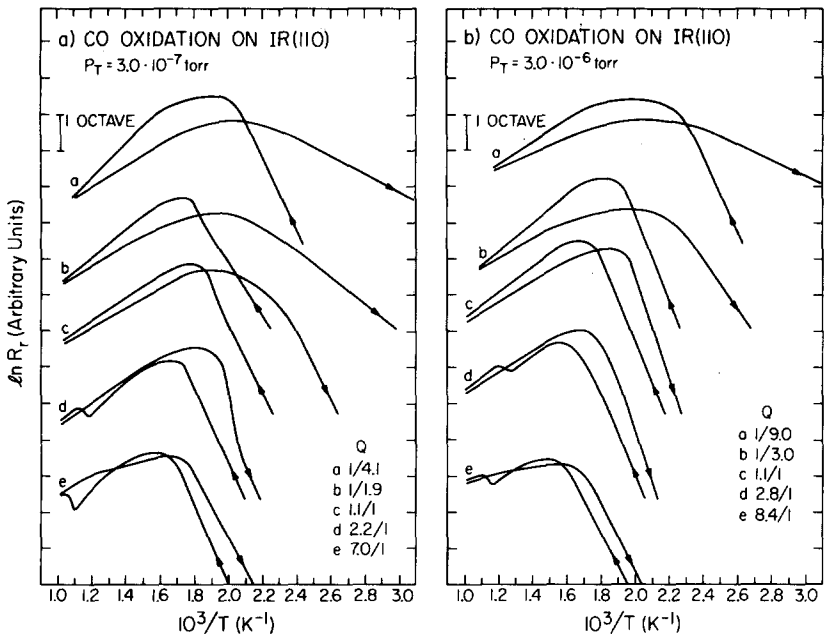

FIG. 3. Arrhenius plots for the variation in the steady-state rates of CO_2 production with surface temperature. Data are shown for various ratios of the partial pressures (Q) and for total pressures of: (a) 3.0×10^{-7}, and (b) 3.0×10^{-6} Torr. The arrows on the curves point to the left if the temperature is increasing and to the right if the temperature is decreasing.

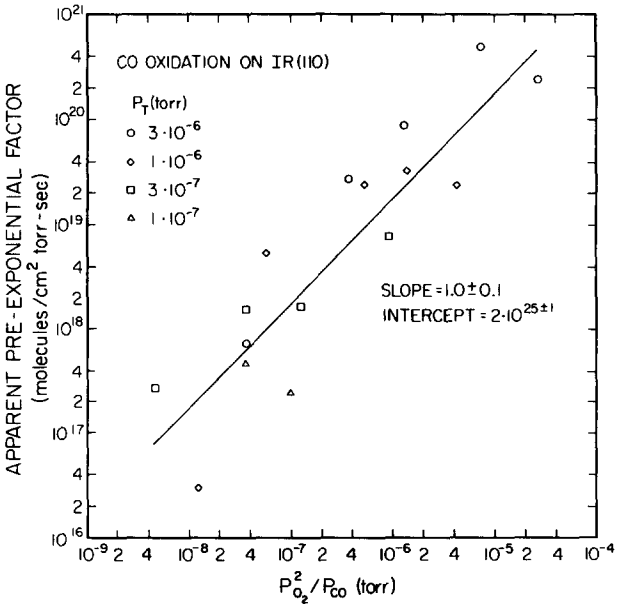

FIG. 4. The variation in the apparent preexponential factor with the ratio of the square of the oxygen pressure to the CO pressure. The apparent preexponential factors were derived from plots similar to those in Fig. 3 and pertain to the region where the apparent activation energy is positive. Only points associated with an increasing surface temperature are shown.

$$R_{r1} = \nu_1(P_{O_2}^2/P_{CO})\exp[-E_1/RT], \quad (3)$$

where E_1 is between 13 and 16 kcal mole^{-1}, and ν_1, from the intercept of Fig. 4, is $2 \times 10^{25\pm1}$ molecules cm^{-2} Torr^{-1} s^{-1}. The scatter in the data of Fig. 4 is not surprising since an error of 2 kcal mole^{-1} in E_1 causes a tenfold variation in ν_1. The apparent preexponential factors were proportional to P_TQ and $P_{O_2}^{3/2}$ also, but these correlations fit poorly at the extremes in the abscissa. In the region where the rate increased with temperature on the oxidized surface, no correlation could be found since the apparent activation energy varied markedly with the partial pressures of the reactants.

In the region where the rate decreases with the temperature of the clean or oxidized Ir(110) surface, the apparent preexponential factor is proportional to P_{CO}, as shown in Fig. 5. There, the factors for the clean surface are shown as empty symbols, whereas the factors for the oxidized surface are shown as filled symbols. No other correlation in the form of Eq. (2) that fits the data could be found. For this temperature regime, the oxidation rate (R_{r_2}) is given by

$$R_{r_2} = \nu_2 P_{CO} \exp[-E_2/kT], \quad (4)$$

where E_2 is between -6 and -3 kcal mole^{-1}, and ν_2, from the intercept of Fig. 5, is $2 \times 10^{19\pm1}$ molecules cm^{-2} Torr^{-1} s^{-1}.

As is clear from Fig. 3, Eqs. (3) and (4) intersect at temperatures near the maximum in the steady-state oxidation rate. If the intersection coincides exactly with the maximum, the temperature at the maximum (T_{max}) would be a function of $Q(= P_{CO}/P_{Ow})$ only, and it would be given implicitly by

$$Q^2 = \nu_3 \exp[-E_3/kT_{max}], \quad (5)$$

where ν_3 is equal to ν_1/ν_2 or approximately $10^{6\pm2}$, and E_3 is equal to $(E_1 - E_2)$, approximately 19 ± 3 kcal mole^{-1}. This equation does not predict T_{max} correctly since T_{max} is to the left of the intersection for values of Q less than 2 and is to the right of the intersection for values of Q greater than 2. However, as shown in Fig. 6, a plot of ln Q as a function of T_{max}^{-1} gives approximately lines

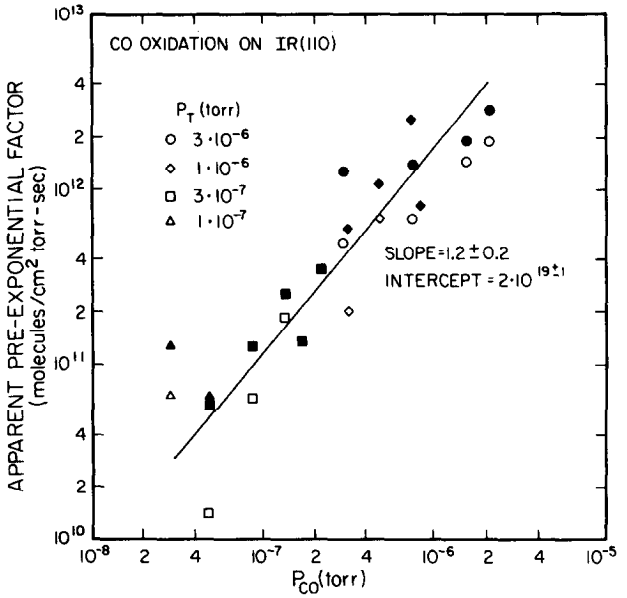

FIG. 5. The variation in the apparent preexponential factor with the partial pressure of CO. The apparent preexponential factors were derived from plots similar to those in Fig. 3 and pertain to the region where the apparent activation energy is negative. Points associated with an increasing surface temperature are hollow whereas points associated with a decreasing surface temperature are solid.

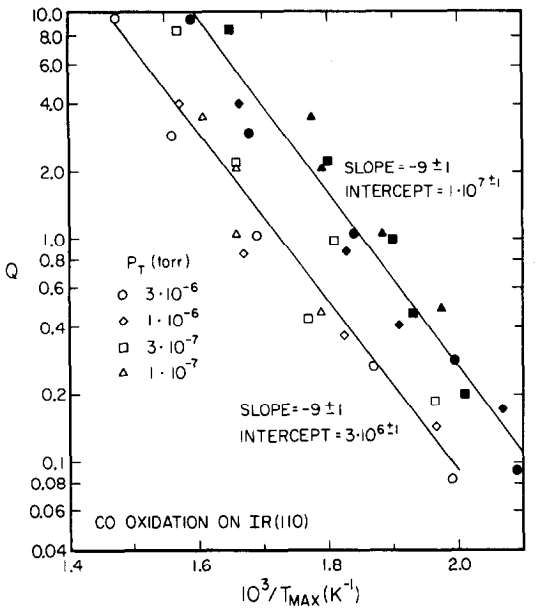

FIG. 6. The variation in the partial pressure ratio $Q(= P_{CO}/P_{O_2})$ with the reciprocal of the temperature associated with the maximum steady-state rate of CO_2 production. Points pertaining to clean Ir(110) are hollow whereas points pertaining to oxidized Ir(110) are solid.

for both clean and oxidized Ir(110). There, points for the respective surfaces are empty and filled. In either case, the slope is -9000 ± 1000 K, which is nearly equal to E_3/k. Also, the intercepts, 3×10^6 for the clean surface and 1×10^7 for the oxidized surface, are nearly equal to ν_3. Hence, the temperature at the maximum in the steady-state rate is approximated by Eq. (5) if the exponent of Q is changed from 2 to 1. Moreover, the rate at the maximum is generally within a factor of 2 lower than the rate given by the intersection of Eqs. (3) and (4).

4. KINETIC MODEL OF STEADY-STATE OXIDATION RATES

A kinetic model will be developed to interpret the steady-state oxidation rates in light also of the transient studies presented elsewhere (*14*). The rates of three elementary reactions—the desorption of CO_2, the desorption of oxygen, and the oxidation of CO via the E–R mechanism—are not included in this model. In the temperature range where the steady-state rates were measured, the rate of CO_2 desorption is extremely rapid and the rate of oxygen desorption is extremely slow, so that both processes do not affect the overall oxidation rate. Studies with modulated molecular beams (*6, 10, 11*) have shown that CO oxidation over the platinum metals between 300 and 1000 K occurs predominantly through the L–H mechanism, whereas the oxidation rate via the E–R mechanism is undetectable. Moreover, the decrease in the oxidation rate observed above 600 K on Ir(110) cannot be attributed to a decrease in the coverage of oxygen and can be explained only if oxidation occurs by the L–H mechanism.

Four processes—the desorption of CO, the oxidation of CO via the L–H mechanism, the adsorption of CO, and the adsorption of oxygen—may limit the steady-state rate of CO_2 production. The rate expressions for the respective processes, determined from transient experiments (*14*), are given by Eqs. (6), (7), (1), and (8).

$$R_d = -\nu_d(\theta_{CO},\theta_O)C_s\theta_{CO} \exp[-E_d(\theta_{CO},\theta_O)/kT], \quad (6)$$

$$R_r = -\nu_r(\theta_{CO},\theta_O)C_3^2\theta_{CO}\theta_O \exp[-E_r(\theta_{CO},\theta_O)/kT], \quad (7)$$

$$C_s\frac{d\theta_O}{dt} = \frac{2S_0(O_2)P_{O_2}(1-\theta_O)^2(1-\theta_{CO})^2}{(2\pi M_{O_2}kT_g)^{1/2}}. \quad (8)$$

Here, $S_0(O_2)$, θ_O, and M_{O_2} are the initial sticking probability of oxygen, the fractional coverage of oxygen, and the molecular weight of oxygen, respectively. The diffusion of oxygen and CO on the surface also may influence the steady-state rate, but these effects are included empirically in Eqs. (6) and (7). When CO oxidation is proceeding under steady-state conditions, the time derivatives of the oxygen and CO coverages are each zero. That is, the rate of CO oxidation is equal to the rate of oxygen ad-

sorption, and the sum of the rates of CO oxidation and CO desorption is equal to the rate of CO adsorption. Hence, Eqs. (6), (7), (1), and (8) may be reduced to three equations

$$R_r + k_2\theta_{CO} = k_1 P_{CO}(1 - \theta_{CO})^2, \quad (9)$$

$$R_r = k_3 P_{O_2}(1 - \theta_{CO})^2(1 - \theta_O)^2, \quad (10)$$

$$R_r = k_4\theta_O\theta_{CO} \quad (11)$$

in three unknowns—θ_{CO}, θ_O, and R_r. Here,

$$k_1 = (2\pi M_{CO}kT_g)^{-1/2},$$
$$k_2 = \nu_d C_s[\exp -E_d/kT],$$
$$k_3 = 2S_o(O_2)[2\pi M_{O_2}kT_g]^{-1/2},$$
$$k_4 = \nu_r C_s^2 \exp[-E_r/kT].$$

The temperature in the gas phase for the steady-state data is 300 K, $S_o(O_2)$ is approximately equal to 0.25 (*17*), and C_s is 10^{15} cm^{-2}. Hence, the values of k_1 and k_3 are approximately 4×10^{20} and 2×10^{20} molecules cm^{-2} $Torr^{-1}$ s^{-1}, respectively. Average values of ν_d, E_d, ν_r, and E_r that are pertinent for the steady-state data are $10^{5.5\pm0.5}$ s^{-1}, 14–17 kcal $mole^{-1}$, 3×10^{-10} cm^2 s^{-1}, and 12 kcal $mole^{-1}$ (*14*). Although Eqs. (9)–(11) may be solved exactly for the steady-state rate under any conditions, the data are analyzed best by using these equations to describe the asymptotic rates above and below the maximum.

In the region where the steady-state oxidation rate increases with the surface temperature, the reaction rate is limited by the desorption of CO and the competitive adsorption of oxygen and CO (*1–3, 6, 10–13*). In this region, the coverage of oxygen is small and may be ignored in Eq. (10) since chemisorbed CO is present to block sites for oxygen chemisorption. Also, the flux of CO molecules to the surface always exceeds the measured oxidation rate by one or two orders of magnitude. Thus, the desorption rate must be large compared to the oxidation rate. (From the average values of the rate parameters for CO oxidation and desorption, the predicted ratio of the rates is nearly unity between 500 and 1000 K. However, an error of 2 kcal $mole^{-1}$ in either of the activation energies would change the ratio by tenfold, so the experimentally determined rates are more appropriate for interpreting the steady-state data.) If the coverage of oxygen is small, and if the desorption rate of CO substantially exceeds the oxidation rate, Eqs. (9) and (10) reduce to

$$R_r = (k_3\nu_d C_s/k_1)Q^{-1} \exp[-E_d/kT]. \quad (12)$$

In deriving Eq. (12), the coverage of CO was assumed to vary negligibly in temperature and to be near one. These assumptions are appropriate since, as was shown previously (*14*), the variation in the rate resulting from the change in the activation energy with coverage may overshadow completely the variation resulting from coefficients that depend on coverages to integral exponents. Moreover, the coverage of CO is near unity for the onset of the steady-state reaction. Equation (12) is identical to the expression derived by Langmuir (*1*) to describe the oxidation rate on Pt in the same temperature regime. Although the adsorption kinetics given by Eqs. (1) and (8) differ from the expressions used by Langmuir, the same expression describes the steady-state rate in either case since the desorption of CO is rate limiting in both models.

For clean Ir(110), the empirical activation energy from Eq. (3), 13–16 kcal $mole^{-1}$, agrees closely with the predicted value from Eq. (12), 17 kcal $mole^{-1}$, which was estimated from transient experiments, described elsewhere (*14*). However, the predicted and empirical dependences of the rate upon the reactant partial pressures are different. The rate is proportional to the pressure of oxygen in the model expression, but varies as the pressure of oxygen squared in the empirical expression. This squared dependence, which is observed also for CO oxidation over Pd(111) for similar temperatures (*6*), may be related to the diffusion of chemisorbed oxygen. Oxygen diffusion on Ir(110) becomes rapid at temperatures where the oxidation rate becomes

rapid (*17*). Moreover, chemisorbed oxygen must diffuse since the O-$p(2 \times 2)$ and the O-$c(2 \times 2)$ LEED patterns are observed during the steady-state reaction. Oxygen atoms may diffuse in pairs so that the diffusion rate depends upon the square of the coverage (*18*). In the regime where oxygen competes with CO for adsorption sites, the coverage of oxygen is proportional to the pressure of oxygen as indicated by Eqs. (10) and (12). Hence, if the diffusion of oxygen limits the overall oxidation rate, the rate would vary as the square of the partial pressure of oxygen. (This variation in the rate cannot be explained by the reaction being limited to the edges of islands of chemisorbed oxygen atoms, for the rate would then vary as the square root of the oxygen pressure.) Information concerning the kinetics of oxygen diffusion is needed to relate the empirical preexponential factor in Eq. (3) to a predicted value, like that in Eq. (12).

For oxidized Ir(110), no empirical expression for the overall oxidation, similar to Eq. (12), could be found. The data for the oxidized surface were obtained in the part of the hysteresis cycles where the surface temperature is decreasing, rather than increasing, so that the model presented in the previous two paragraphs may not be appropriate for this region. Moreover, the oxide, which is reactive to reduction by CO, may be decomposed partially as the temperature is decreased, but this conjecture was not tested.

In the region where the steady-state rate is decreasing with the surface temperature, the empirical expression for the rate over clean and oxidized Ir(110) [Eq. (4)] may be derived from Eqs. (9)–(11). As determined from desorption rates of CO calculated elsewhere (*14*), the coverage of CO is small for this temperature regime. As shown previously, the desorption rate of CO is much larger than the oxidation rate. Hence, Eq. (9) is approximated closely by $\theta_{CO}k_2 = k_1P_{CO}$. Using this expression to give the coverage of CO, Eq. (11) becomes

$$R_r = (k_1C_s\theta_O\nu_r/\nu_d)P_{CO} \exp[(E_d - E_r)/kT]. \quad (13)$$

Both the activation energy (*6*) and the pressure dependence (*5–7, 19–21*) for the oxidation rate in this expression have been derived previously for other platinum metal catalysts. The coverage of CO is too small to inhibit the adsorption of oxygen, and, as determined from the data in Fig. 1, the oxidation rate is not limited by the flux of oxygen to the surface. Thus, the coverage of oxygen in this temperature regime approaches the saturation value, 0.5 ml. Using the average values for ν_d and ν_r that were given previously, the predicted value of the preexponential factor from Eq. (13), $k_1C_s\theta_O\mu_T/\nu_d = 2 \times 10^{20\pm1}$ molecules cm^{-2} $Torr^{-1}$ s^{-1}, is quite close to the empirical value from Eq. (4), $2 \times 10^{19\pm1}$ molecules cm^{-2} $Torr^{-1}$ s^{-1}. Moreover, the pressure dependences of the two expressions are identical, and the predicted value for the activation energy, -5 to -2 kcal $mole^{-1}$, is quite close to the observed value, -6 to -3 kcal $mole^{-1}$.

CONCLUSIONS

The heterogenously catalyzed reaction of gaseous CO and O_2 to form CO_2 over Ir(110) has been studied through measurements of the steady-state rate of CO_2 production and of the transient kinetics of elementary reactions that may limit the steady-state rate (*14*). Both clean and oxidized Ir(110) were used as catalysts. The surface oxide, which is distinct chemically from chemisorbed oxygen, forms irreversibly at temperatures where the steady-state rate of CO oxidation is rapid. The desorption of CO, the oxidation of CO via the Langmuir–Hinshelwood mechanism, the adsorption of CO, and the adsorption of oxygen may limit the steady-state rate of CO oxidation, whereas the desorption of oxygen, the desorption of CO_2, and the oxidation of CO via the Eley–Rideal mechanism do not affect the rate significantly for catalyst temperatures between 300 and 1000

K. The rates of the four elementary reactions that may limit the steady-state rate depend complexly on the composition of the adlayer. Moreover, the steady-state rate may depend critically upon the diffusion rates of chemisorbed oxygen and CO, which were not measured directly in this study.

Models for the steady-state oxidation rate, based on the rate expressions developed from the transient experiments (*14*), give a consistent interpretation of the rate data for surface temperatures from 300 to 1000 K and for partial pressures of the reactants between 1×10^{-8} and 3×10^{-6} Torr. Below 600 K, where the oxidation rate increases with the surface temperature, the rate is inversely proportional to the partial pressure of CO, but is proportional to the square of the partial pressure of oxygen. The unusual variation in the rate with the oxygen pressure may be associated with the diffusion of chemisorbed oxygen on the surface. If the steady-state rate is measured as the surface temperature is increased below 600 K, the apparent activation energy and preexponential factor for the steady-state rate on clean Ir(110) are 14 ± 2 kcal mole^{-1} and $2 \times 10^{25\pm1}$ molecules cm^{-2} Torr^{-1} s^{-1}. However, if the rate is measured as the temperature is decreased, the apparent activation energy and preexponential factor vary considerably due to hysteresis in the rate of CO_2 production. Since the rates of the elementary reactions that limit the steady-state rate are nonlinear functions of the coverages of CO and oxygen, the Gibbs energy for any surface temperature may have several local minima so that hysteresis may occur. Above 600 K, where the steady-state rate decreases with the surface temperature, the oxidation rate is proportional to the partial pressure of CO, but is independent of the partial pressure of oxygen. Regardless of whether the surface is clean or oxidized, and whether the surface temperature is being increased or decreased, the apparent activation energy and preexponential factor for the overall rate coefficient are -4 ± 2 kcal mole^{-1} and $2 \times 10^{19\pm1}$ molecules cm^{-2} Torr^{-1} s^{-1}. The temperature associated with the maximum oxidation rate at steady state occurs near the intersections of the asymptotic curves above and below 600 K, and it is inversely proportional to the logarithm of the ratio of the CO partial pressure to the oxygen partial pressure.

REFERENCES

1. Langmuir, I., *Trans. Faraday Soc.* **17**, 621 (1922).
2. Ertl, G., and Rau, P., *Surface Sci.* **15**, 443 (1969).
3. Bonzel, H. P., and Ku, R., *J. Vac. Sci. Technol.* **9**, 663 (1971).
4. Christmann, K., and Ertl, G., *Z. Naturforsch. A* **28a**, 1144 (1973).
5. Close, J. S., and White, J. M., *J. Catal.* **36**, 185 (1975).
6. Engel, T., and Ertl, G., *J. Chem. Phys.* **69**, 1267 (1978).
7. Golchet, A., and White, J. M., *J. Catal.* **53**, 266 (1978).
8. Heyne, H., and Tompkins, F. C., *Proc. Royal Soc. A* **292**, 460 (1966).
9. Winterbottom, W. L., *Surface Sci.* **36**, 205 (1973).
10. Palmer, R. L., and Smith, J. N., Jr., *J. Chem. Phys.* **60**, 1453 (1973).
11. Pacia, N., Cassuto, A., Pentenero, A., and Weber, B., *J. Catal.* **41**, 455 (1976).
12. Zhdan, P. A., Boreskov, G. K., Egelhoff, W. F., Jr., and Weinberg, W. H., *Surface Sci.* **61**, 377 (1976).
13. Ivanov, V. P., Boreskov, G. K., Savchenko, V. I., Egelhoff, W. F., Jr. and Weinberg, W. H., *J. Catal.* **48**, 269 (1977).
14. Taylor, J. L., Ibbotson, D. E., and Weinberg, W. H., Submitted.
15. Taylor, J. L., Ph.D. thesis, California Institute of Technology, 1978.
16. Taylor, J. L., Ibbotson, D. E., and Weinberg, W. H., *J. Chem. Phys.* **69**, 4298 (1978).
17. Taylor, J. L., Ibbotson, D. E., and Weinberg, W. H., *Surface Sci.* **79**, 349 (1979).
18. Thiel, P. A., Yates, J. T., Jr., and Weinberg, *Surface Sci.* **82**, 22 (1979).
19. Matsushima, T., and White, J. M., *J. Catal.* **39**, 265 (1975).
20. Matsushima, T., Almy, D. B., and White, J. M., *Surface Sci.* **67**, 89 (1977).
21. Matsushima, T., and White, J. M., *Surface Sci.* **67**, 122 (1977).